Chemical Engineering Science 138 (2015) 375–384

Contents lists available at ScienceDirect

Chemical Engineering Science

journal homepage: www.elsevier.com/locate/ces

Oxidative protein refolding on size exclusion chromatography: From batch single-column to multi-column counter-current continuous processing

Pegah Saremirad [a], Jeffery A. Wood [b], Yan Zhang [c], Ajay K. Ray [a,*]

[a] Department of Chemical and Biochemical Engineering, University of Western Ontario, London, Canada
[b] Soft Matter, Fluidics and Interfaces, MESA+ Institute for Nanotechnology, Faculty of Science and Technology, University of Twente, Enschede, The Netherlands
[c] Faculty of Engineering & Applied Science, Memorial University of Newfoundland, St John's, Canada

HIGHLIGHTS

- Mathematical model presented for its applicability for protein oxidative refolding/aggregation predictions in SMB-SEC.
- The model considers a wider loading concentration range of the model protein (lysozyme) on SEC.
- It was observed that at higher loading concentrations aggregation occurs when local protein concentration exceeds a critical concentration.
- The model was found to predict the SMB-SEC performance of solubilized protein recovery.
- No urea recovery at the product stream indicated that the refolding reaction will continue off-column to recover the native-protein product.

ARTICLE INFO

Article history:
Received 11 May 2015
Received in revised form
13 August 2015
Accepted 23 August 2015
Available online 8 September 2015

Keywords:
Intensified protein refolding
Size exclusion chromatography
Mathematical modeling
Off-column refolding

ABSTRACT

Recently protein refolding on size exclusion chromatography (SEC) operated in multi-column continuous simulated moving bed (SMB) configurations (hereinafter SMB-SEC) has been investigated for future industrial applications. This is due to several advantages offered by SMB configurations particularly when process parameters are thoroughly screened and optimized. A robust mathematical model is essential for high-throughput process screening and optimization. In this work, a previously investigated single-column mathematical model was modified to extend its applicability for protein oxidative refolding/aggregation predictions in SMB-SEC. The model considers a wide loading concentration range of the model protein (lysozyme) on SEC. The potential influences of high concentrations of chaotropic reagents on kinetic and thermodynamic model parameters have been discussed based on previous experimental results and their predicted local concentrations through the SMB-SEC columns and at the product stream. It was observed that aggregation occurs when local protein concentration exceeds a critical concentration. No urea recovery at the product stream indicated that the refolding reaction will continue off-column to recover the native-protein product. Therefore, it is suggested that the developed model is tested against experimental results for total soluble protein (early intermediates and native conformations) in the presence of L-arginine additive and process performance indicators are defined based on this criterion.

1. Introduction

Despite the advances made to date for expression of protein-therapeutics using *Escherichia coli* (Huang et al., 2012), existing technologies to recover active and high-purity product still incur significant costs due to low product concentration and high buffer consumption during conventional batch dilution refolding process resulting in low volumetric productivity (Freydell et al., 2011). As

* Corresponding author. Fax: +1 519 661 3498.
E-mail address: aray@eng.uwo.ca (A.K. Ray).

http://dx.doi.org/10.1016/j.ces.2015.08.031
0009-2509/

an alternative, SEC has been widely used at lab scale (Freydell et al., 2011; Freydell et al., 2010a; Gu et al., 2001; Lanckriet and Middelberg, 2004; Park et al., 2006; Wellhoefer et al., 2014, 2013). Due to the gradual separation of denaturing and reducing agents from unfolded protein molecules and their separation from soluble aggregates, SEC allows for higher working concentrations compared to dilution refolding and results in high refolding yield and purity. However, this method in form of single-column batch processing may not enhance the process performance indicators (e.g. productivity and buffer consumption) for industrial scale production of *E. Coli*-based protein-therapeutics. On the other hand, a multi-column continuous simulated moving bed system offers several advantages compared to single-column batch operation including increased productivity per unit mass of solid phase, lower solvent consumption, and less diluted products. This configuration consists of a set of chromatographic columns connected in series and is operated in continuous mode; the inlet/outlet lines are periodically shifted synchronously in the direction of liquid-phase flow to mimic countercurrent movement between a liquid-solvent and a solid phase. Multi-column continuous simulated moving bed is a well-established process for intensified difficult separations of small molecules and fine products e.g. separation of enantiomers (Rajendran et al., 2009; Ströhlein et al., 2005). However, its application for protein refolding and separation has recently attracted the attention of researchers (Freydell et al., 2010b; Park et al., 2006; Wellhoefer et al., 2014, 2013). For example, Freydell et al. have reported a 35 times increase in productivity and 1/10th solvent consumption when a SMB-SEC was used for refolding of a model fusion protein compared to single-column processing.

Since many parameters are involved in operating a SMB-SEC (i.e. internal and external flow rates, switching time and feed concentration) systematic optimization studies are required to exploit the full potential of this system. A mathematical model is a pre-requisite for screening of process parameters and optimization. Freydell et al. used a previously investigated single-column model in order to predict refolding/aggregation of a fusion protein in a four-zone SMB-SEC configuration comprised of multiple columns connected in series. They observed considerable discrepancy between model predictions and experimental results based on native refolded protein recovery. For instance, the refolding yield was over-predicted by a factor of three. As discussed in the same work, this disagreement can be related to lower dilution factor in SMB-SEC compared to a batch single-column refolding resulting in higher local concentration of chaotropic agents (urea and DTT). And, in order to improve the SMB-SEC model- predictions in terms of native protein recovery the influence of local concentration of urea and DTT on model parameters should be considered.

The effect of lower dilution factor is twofold, as in addition to higher local concentrations of chaotropic reagents it also results in higher local protein concentration compared to a batch single-column refolding. Higher local protein concentration may additionally result in different reaction schemes. For example if for a single-column refolding experiment no aggregation was observed there would still remain the possibility of aggregation in SMB-SEC at the same protein loading concentrations.

In this work, (1) a previously experimentally verified single-column model was modified to expand its applicability for prediction of oxidative protein refolding/aggregation on SMB-SEC by considering a wide protein loading concentration range (i.e. low loading concentrations where no aggregation was observed and high loading concentrations where aggregation occurred) and the additional model parameters resulting from this modification were determined experimentally. The approach presented in this work is different from that of existing research work where only high loading concentrations are considered to model protein refolding/aggregation; (2) the sensitivity of refolding kinetics and possible complexity arising from reducing agent (DTT) carry-over have been discussed and DTT-free refolding was investigated and compared to previous studies with DTT carry-over; (3) the denaturing reagent (urea) mass transfer parameters were measured experimentally and used to predict the concentration of urea through SMB-SEC columns and at the product outlet under the current operation conditions; (4) the suitability of the developed model for process optimization was explored and an appropriate criterion for model validation was proposed; and (5) the effect of SMB-SEC operating parameters namely loading concentration and switching time on process performance indicators were predicted and the results were compared to single-column oxidative refolding of lysozyme.

2. Mathematical model and theory

2.1. Column model

The protein refolding in size exclusion column was modeled using dispersive transport in the bulk with a film linear mass transfer resistance between particle-solid and bulk-liquid phases. The formulated differential mass balances for solutes in the bulk and the solid phases are (Freydell et al., 2010a)

$$\frac{\partial C_{b,i}}{\partial t} = D_L \frac{\partial^2 C_{b,i}}{\partial x^2} - u\frac{\partial C_{b,i}}{\partial x} - Pk_{ov,i}\left(C_{eqS,i} - C_{s,i}\right) + r_{b,i} \tag{1}$$

$$\frac{\partial C_{s,i}}{\partial t} = k_{ov}\left(C_{eqS,i} - C_{s,i}\right) + r_{s,i} \tag{2}$$

where $C_{b,i}$ and $C_{s,i}$ are the concentration of solute i (unfolded, intermediates and native conformations) in bulk and solid phase respectively. Note that in Eq. (1), the total concentration of species is constant. In Eqs. (1) and (2), $t$represents time, x axial distance along the column, D_L axial dispersion coefficient, u interstitial velocity, $k_{ov,i}$ solute overall mass transfer coefficient, P phase ratio, $C_{eqS,i}$ the solid phase concentration in equilibrium with the bulk concentration. $r_{b,i}$ and $r_{s,i}$ are the net concentration change due to refolding and aggregation reactions in bulk and solid phases, which are described further in Section 2.3.

The solute solid phase concentration in equilibrium with the bulk concentration was treated as a linear equilibrium relationship with a fixed equilibrium constant (Zelic and Nesek, 2006):

$$C_{eqS,i} = K_{eq,i} C_{b,i} \tag{3}$$

where $K_{eq,i}$ is the equilibrium constant.

The boundary and initial conditions used to solve Eqs. (1) and (2) are as follows:

$$C_{b,i}\left(t, 0^-\right) = \begin{cases} C_{f,i} & 0 < t < t_{pulse} \\ 0 & t > t_{pulse} \end{cases} \tag{4a}$$

$$\frac{\partial C_{b,i}}{\partial x}(t, L_C) = 0 \tag{4b}$$

$$C_{b,i}(0, x) = 0 \tag{4c}$$

$$C_{s,i}(0, x) = 0 \tag{4d}$$

where $C_{f,i}$ is solute concentration in feed, t_{pulse} is the duration of sample injection, and L_C is the column length. The assumption that

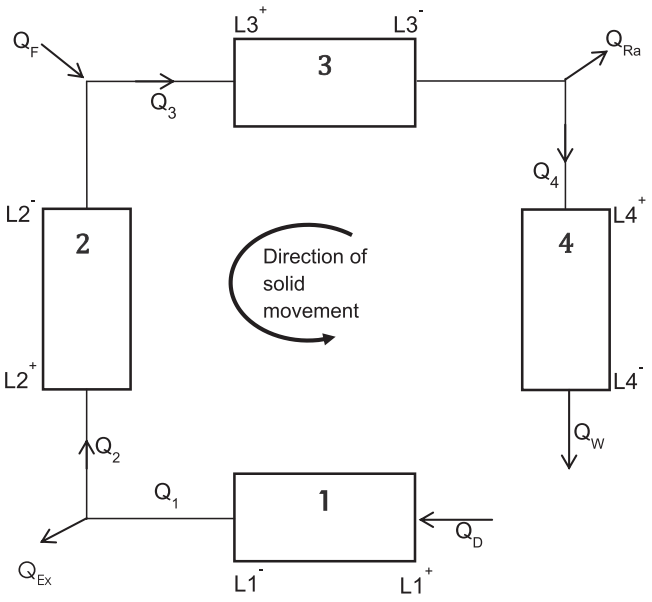

Fig. 1. Schematic representation of a four-zone SMB-SEC: Q_D, Q_{Ex}, Q_{Ra}, Q_F and Q_W are buffer, extract, raffinate, feed and waste flow rates respectively. Q_j is internal flow rate in zone j: 1–4).

the sample is introduced into the column as a rectangular pulse of length t_{pulse} was initially used as it has proven applicable in some cases (Freydell et al., 2010a; Zhang et al., 2008). However, the experimental injection profile was later introduced by a Gaussian distribution function to further improve the accuracy of the model parameters and prediction results.

To solve the $C_{b,i}$ and $C_{s,i}$ along x at different times, the first and second spatial derivatives were discretized as fourth-order central finite difference equations except for boundary points where second order forward and backward finite difference approximations were used. The resulting system of ODEs in time (method of lines) was solved numerically in MATLAB using the solver ode15s.

2.2. SMB-SEC model

The selected design parameters of SBM-SEC model (e.g. number of columns in each zone and column dimensions) in this work were identical to the system used by Freydell et al. (2010b). Fig. 1 shows a schematic representation of their system. Each zone comprises of two columns connected in series and as shown on the same figure an open loop system was used. The dimension of each column is 1 cm i.d and packed bed height of ~8 cm. Each column was modeled with the same approach as for single column except that boundary conditions are taken as periodic. The changing boundary condition is simulated by hypothetical movement of solid (direction shown on Fig. 1) or more accurately switching columns' positions after each switching time. The boundary condition for each node is then:

$$C_{b,i}\left(t, L_1^+\right) = C_{D,i} \tag{5a}$$

$$C_{b,i}\left(t, L_2^+\right) = C_{b,i}\left(t, L_1^-\right) \tag{5b}$$

$$C_{b,i}\left(t, L_3^+\right) = \frac{Q_F C_{f,i} + Q_2 C_{b,i}\left(t, L_2^-\right)}{Q_3} \tag{5c}$$

$$C_{b,i}\left(t, L_4^+\right) = C_{b,i}\left(t, L_3^-\right) \tag{5d}$$

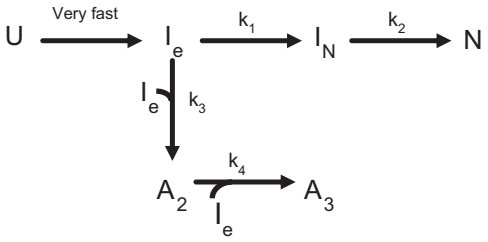

Fig. 2. Lysozyme refolding and aggregation kinetic scheme, U: unfolded protein I_e: early intermediates, I_N: native-like intermediates, N: native protein, and A_n: aggregates (n: 2 and 3).

where $C_{D,i}$ is the concentration of component i in the refolding buffer.

2.3. Reaction scheme

The refolding of reduced/denatured lysozyme has been successfully modeled using a single dominant reaction pathway in batch and fed batch refolding (Buswell and Middelberg, 2003; Goldberg et al., 1991). The reaction mechanism is shown in Fig. 2. It is suggested that early intermediates with only a small fraction of disulfide bridges are rapidly formed during "collapse process", followed by formation of native-like intermediates and a slow conversion of these intermediates to native state (van den Berg et al., 1999). Since early intermediates are more susceptible to aggregation compared to native-like intermediates, aggregation is considered the result of early intermediate species association via sequential polymerization mechanism (Buswell and Middelberg, 2003; Freydell et al., 2010a; Goldberg et al., 1991). In our previous work, lysozyme refolding on SEC could be well described by an apparent two state mechanism involving early intermediates and native lysozyme (Saremirad et al., 2014b). Furthermore when lysozyme was refolded without L-arginine additive, only one size of soluble aggregates was recovered (Saremirad et al., 2014a), therefore it was assumed that only one size of aggregate is also formed in the presence of L-arginine and aggregation was then regarded as a second order reaction. According to this simplified scheme the reaction rates for bulk ($r_{b,i}$) and solid ($r_{s,i}$) phases in Eqs. (1) and (2) are as follows:

$$r_{I_e} = -k_{app} C_{I_e} - 2\, k_a (C_{I_e})^2 \tag{6a}$$

$$r_{I_N} = k_{app} C_{I_e} \tag{6b}$$

$$r_{A_2} = k_a (C_{I_e})^2 \tag{6c}$$

where k_{app} and k_a are apparent refolding and aggregation kinetic constants respectively.

Aggregation occurs at higher local concentrations which might be purely due to increased aggregation kinetics competing with refolding reaction or surpassing early refolding kinetic species solubility (Ricchiuto et al., 2012). In the former case, the thermodynamic condition for aggregation formation is always satisfied while for the latter there is a critical concentration above which aggregates are formed. Elution profiles of refolded native protein for lysozyme refolding on SEC for a wide protein loading concentration range (5–50 mg/mL) are examined in this work to investigate both case scenarios, assessed through inclusion of these effects in the model through an aggregation kinetic constant (k_a) and early intermediate solubility (C_s).If a critical concentration is required to describe the results of refolding/aggregating on SEC,

the aggregation rate is modeled as follows:

$$r_{A_2} = \begin{cases} k_a(C_{l_e})^2 & C_{l_e} \geq C_s \\ 0 & C_{l_e} < C_s \end{cases} \quad (6d)$$

2.4. Model parameters estimated by single-column experiments

In our previous work an axial dispersion coefficient was calculated using available correlations for packed bed columns. Also, the void volume, which was necessary for axial dispersion coefficient and phase ratio calculations, was measured using thyroglobulin from bovine thyroid as a test probe. Furthermore, the mass transfer and equilibrium constants for early intermediates and native lysozyme ($k_{ov,i}$ and $K_{eq,i}$) were found by least-squares fitting of the deviation of measured concentration during single-column experiments vs. calculated for BSA model protein and native lysozyme respectively. The refolding kinetic constant (k_{app}) was also obtained in the same manner for elution profile of refolded native lysozyme when low loading concentrations (5–20 mg/mL) of denatured/reduced lysozyme were refolded on SEC. Low loading concentrations were used to prevent aggregation (Saremirad et al., 2014b).

In this work, in order to introduce aggregation into the model, the aggregation kinetic constant (k_a) and early intermediate solubility (C_s), were determined by least square fitting of measured refolded native protein concentration vs. calculated (Eq. 7) accomplished via the fminsearch function of MATLAB to find the parameters which indicated a global minimum

$$f(x) = \sum_{j=1}^{j=n} (C_{b,i}^{exp,j} - C_{b,i}^{fit,j}(x))^2 \quad (7)$$

The above kinetic and thermodynamic parameters vary depending on local concentration of urea and DTT. In order to investigate the concentration profile of urea in SMB-SEC, mass transfer and equilibrium constants were found by measuring the concentration profile of pure urea injection on single column and minimization of deviation of experimental vs. predicted results. The correlations for these constants have found to have wide errors as shown in the work of Park et al. (2006), which motivated experimental determination of these values.

2.4.1. Effect of denaturant and reducing agents on model parameters

The carry-over of both urea and DTT, present in the feed stream, to the refolding environment can influence the results of refolding. However, it should be noted that DTT exists in both oxidized and reduced forms, which each possess different effects on refolding and aggregation kinetics. Concentrations equal or higher than of 0.6 mM of reduced form of this reagent can completely stop the refolding of lysozyme, while both the reduced and oxidized forms might result in non-optimal redox couple concentration ratio and indirect adverse effects (Lanckriet and Middelberg, 2004). Furthermore, the oxidized to reduced ratio of this reducing agent will change over time due to oxidation unless continuous feed preparation is implemented. The oxidized to reduced ratio is also dependent on the feed protein concentration as the protein concentration varies whereas the initial concentration of DTT in the feed is constant. For the above mentioned reasons the task quantifying the different effects becomes challenging. DTT may be removed before introducing the feed stream to the continuous refolding system. In order to gain more information on possible effects of DTT removal, batch single-column experiments of DTT-free lysozyme refolding were executed and the results were compared to the cases with carry-over of DTT.

The concentration profile of urea in SMB-SEC was predicted to find out more information about its local concentrations through the columns and separation from unfolded lysozyme. Since the purpose was to study the urea and protein concentration-waves separation, no reaction was considered. This investigation assisted in deciding whether further experimentations are required to find suitable functions to related kinetics of on-column refolding, aggregation and solubility to urea local concentrations.

3. Materials and methods

3.1. Chemicals

Reagent grade L-arginine and urea, Ethylene Diamine Tetra Acetic acid (EDTA), lysozyme from chicken egg white, trizma® base (Tris-base), cysteine, cystine, BioUltradithiothreitol (DTT) solution, Trifluoric acetic acid (TFA) reagent plus grade and acetonitrile 0.1% TFA were purchased from Sigma-Aldrich, Canada. DIUR-500 urea assay kit and Red 660™ protein assay reagent were purchased from Bioassays, and G-Biosciences, USA respectively. Superdex™ 75 pg resin (34 μm average particle size) was purchased from GE healthcare, Canada.

3.2. Analytical methods

3.2.1. Native protein concentration

A Vydac 214MS C_4 column (5 μm, 250 × 4.6 mm^2) was used on an Agilent HPLC system to separate native protein from other protein conformations and determine its concentration in samples collected during protein refolding experiments on SEC. A linear acetonitrile-water gradient with 0.1% (v/v) TFA starting at 25% acetonitrile increasing at 2.3%/min was used to elute the protein in 10 min. The total solvent flow rate, column temperature and injection volume were set at 1 mL/min, 20 °C and 50 μL respectively.

Concentration of native protein in samples collected during injection profile determination was calculated by comparing the UV absorbance of samples and native protein standards at 280 nm. Both standards and samples UV absorbance reading were carried in a Tecan M200 plate reader.

3.2.2. Total protein concentration

The total protein concentration in protein pool after DTT removal was determined with Red 660™ protein assay using microtiterplate reader in which 10 μl protein samples were transferred to each well, 150 μL of reagent were added and mixed using the plate reader (6.5 mm circular shaker), and absorbance of the mixture at 660 nm was measured after 5 min. The total protein concentrations were calculated by comparing the fraction and standard protein sample absorbance.

3.2.3. Urea concentration

The urea concentrations in samples were determined by urea assay kit (DIUR-500) using microtiterplate reader in which 5 μl of diluted samples were transferred to each well, 200 μL of reagent were added and mixed using the plate reader (6.5 mm circular shaker), and absorbance of the mixture at 520 nm was measured after 20 min. The samples were diluted with water instead of refolding buffer to avoid the interference of L-arginine with the assay (as recommended by the manufacturer).

3.3. Protein unfolding

Unfolding buffer (0.1 M Tris-base, 1 mM EDTA, 6 M urea and 32 mM DTT, pH 8.1) was used to prepare various concentrations of denatured/reduced lysozyme. The sample was incubated for 2–4 h

at 37 °C for lysozyme concentrations under 20 mg/mL (Lanckriet and Middelberg, 2004) and above 30 mg/mL respectively. The loss of native structure was confirmed by RP-HPLC analysis afterwards.

3.4. Protein injection profile

The injection profile of protein was determined by replacing the column on ÄKTA purifier 100 by a piece of tubing with the same dimensions as column inlet tubing. The same injection loops were used for manual loading of native protein sample dissolved and eluted with refolding buffer. Fractions of 200 μl were collected and the concentration of native protein for each fraction was determined using UV absorbance.

3.5. DTT removal

A 5 mL Hitrap desalting column (GE healthcare) was used to remove DTT from denatured/reduced lysozyme. The column was equilibrated with 2 CVs of unfolding buffer without DTT (0.1 M Tris-base, 1 mM EDTA, 6 M urea). 0.5 mL samples of 25 mg/mL were injected on column and eluted with 1 mL/min flow rate of unfolding buffer. Fractions of 0.5 mL were collected and pooled for refolding experiments described in the next section. In order to investigate the refolding of higher concentration of DTT-free lysozyme, the pool of desalting stage was concentrated using 10 K 4 mL Amicon® Ultra-centrifugal filters. The pool total protein concentration was determined using total protein assay as described above.

3.6. Single-column batch refolding

A XK16/40 column (GE healthcare, Canada) packed with Superdex™75 prep grade resin (column volume ~54 mL) was installed on ÄKTA purifier 100 controlled by UNICORN 5.31 software and equipped with online pH probe, UV detector and conductivity cell. The fractionation kit allows the collection of samples at desired volumes. Acetone pulse injection (2% (v/v)) was used to test the packing quality by comparing the peak symmetry and number of theoretical plates per length of column with manufacturer recommended criteria.

The column was equilibrated with 2 CVs of the refolding buffer (0.1 M Tris, 1 mM EDTA, 2 M urea, 0.2 M L-arginine, 3 mM cysteine, 0.3 mM cysteine buffered at pH 8.1) prior to injection of 1 mL of denatured/reduced lysozyme with various concentrations (30, 40 and 50 mg/mL). The sample was eluted using the same buffer and flow rate of 1 mL/min. Fractions of 1 mL were collected and concentrations of native protein were determined using RPHPLC. The same procedure was followed for refolding of denatured/reduced lysozyme after DTT removal.

3.7. Early intermediate-solubility test

Samples of 40 mg/mL DTT-free lysozyme in 0.1 M Tris-base, 1 mM EDTA, 6 M urea buffered at pH 8.1 were diluted using a Tris-base buffer pH 8.1containing urea and L-arginine without redox couple. The urea and L-arginine concentrations were adjusted to result in a buffer identical to refolding buffer used during on-column refolding experiments considering the dilution factor. The absence of redox couple quenches the reaction at early intermediates (Saremirad et al., 2014a, 2014b). DTT was removed for the same reason to avoid the formation of native protein during dilution experiments. The initial concentration of diluted sample was 8 mg/mL which was incubated overnight. The aggregates were precipitated using a centrifuge and the concentration of soluble protein in supernatant was measured by total protein assay.

3.8. Urea injection

A sample of 6 M urea was prepared in a buffer similar to the refolding buffer composition with the exception of urea. No urea was used in this buffer to avoid high dilution factors during urea concentration measurements. 0.5 mL of this sample was injected on the SEC column and eluted with 1 mL/min flow rate of the same buffer while collecting fractions of 1 mL. The experimental elution profile of urea was obtained by measuring urea concentration in the samples using urea assay kit.

3.9. SMB-SEC Simulations

After determining the necessary model parameters, the SMB-SEC operational parameters (i.e. external and internal flow rates and switching time) were selected using triangle theory. Based on this theory, inequalities of (8)a–(8)c correspond to a design space where complete separation can be achieved (Mazzotti et al., 1997)

$$K_{eq,urea} < m_1 < \infty \tag{8a}$$

$$K_{eq,\,N} < m_2 < m_3 < K_{eq,urea} \tag{8b}$$

$$\frac{-\varepsilon_p}{(1-\varepsilon_p)} < m_4 < K_{eq,urea} \tag{8c}$$

where m_j is called phase flow rate ratio and defined as ratio of net liquid flow rate to net solid phase flow rate in zone j and ε_p is particle porosity. Particle porosity was measured experimentally using acetone and thyroglobulin from bovine thyroid injections on single column. Acetone and thyroglobulin from bovine thyroid elution volume to total column volume ratios measure total porosity (ε) and void volume (ε_b) respectively and the particle porosity is calculated as: $\varepsilon_p = \frac{\varepsilon-\varepsilon_b}{1-\varepsilon_b}$ (Freydell et al., 2010b). Total bed porosity, void volume fraction and total particle porosity were found to be 0.92, 0.34 and 0.88 respectively. The equilibrium constants for native lysozyme and urea were found by least-squares fitting of the deviation of measured concentration vs. calculated for native protein and urea when native lysozyme and pure urea were injected on the single column. The fitted parameters are 0.9 for urea and 0.44 for native lysozyme (Saremirad et al., 2014a, 2014b). The liquid flow rate in each SMB-SEC zone is related to phase flow rate ratio by the following:

$$Q_j = \frac{m_j V_c(1-\varepsilon) + V_c\varepsilon}{t_s} \tag{9}$$

where t_s is the switching time.

In addition to the above criteria the flow rates must be within lowest and the highest flow rate range which are considered 0.25 and 3 mL/min respectively. For the selected flow rate range, Young and Wilson–Geankoplis correlations (Freydell et al., 2010a) were used to determine the controlling mass transfer resistance by order of magnitude analysis which revealed the pore resistance as the major resistance component. Since this value is independent of the velocity the estimated model parameters are valid for the selected flow rate range. The highest flow rate is determined based on maximum allowable pressure over the system compatible with packing and column material. Table 1 reports the operational parameters which were used during SMB-SEC simulations.

The continuous and batch process performance indicators are defined as follows:

$$R_{b,exp} = \frac{M_{soluble}}{LV_{pulse}} \tag{10a}$$

$$R_{c,pred} = \frac{C^{CSS}_{soluble.Ra} Q_{Ra}}{Q_F C_{f,U}} \tag{10b}$$

where $R_{b,exp}$ and $R_{c,pred}$ are experimental and predicted soluble lysozyme recovery for batch and continuous refolding respectively. $M_{soluble}$ is sum of soluble protein mass collected in fractions, V_{pulse} injection volume, L lysozyme loading concentration and $C^{CSS}_{soluble.Ra}$ predicted average concentration of soluble protein at cyclic steady state

Table 1
SMB-SEC operational parameter selected based on triangle theory.

Phase flow rate ratios	t_s (min)	$Q_D = Q_1$ (mL/min)	Q_2 (mL/min)	Q_3 (mL/min)	$Q_4 = Q_W$ (mL/min)	Q_{Ex} (mL/min)	Q_F (mL/min)	Q_{Ra} (mL/min)
$m_1 = 1.3$	2.7	2.72	1.66	1.96	1.21	1.04	0.30	0.74
$m_2 = 0.6$	3	2.39	1.47	1.74	1.08	0.92	0.26	0.66
$m_3 = 0.8$	3.3	2.17	1.34	1.58	0.98	0.84	0.24	0.64
$m_4 = 0.3$								

$$Pr_{b,exp} = \frac{M_{soluble}}{V_C t_e} \tag{11a}$$

$$Pr_{c,pred} = \frac{C^{CSS}_{soluble.Ra} Q_{Ra}}{N_t V_C} \tag{11b}$$

where $Pr_{b,exp}$, $Pr_{c,pred}$, t_e, V_c, and N_t are experimental and predicted volumetric productivity for batch and continuous configurations, elution time of protein for batch experiments, volume of the column and total number of columns used for SMB-SEC respectively

$$P_{c,pred} = \frac{C^{CSS}_{soluble.Ra}}{C^{CSS}_{soluble.Ra} + C^{CSS}_{urea.Ra}} \tag{12}$$

$P_{c,pred}$ is the predicted product purity

$$Bc_{b,exp} = \frac{Qt_e}{M_{soluble}} \tag{13a}$$

$$Bc_{c,pred} = \frac{Q_D}{C^{CSS}_{Soluble.Ra} Q_{Ra}} \tag{13b}$$

where $Bc_{b,exp}$ and $Bc_{c,pred}$ are experimental and predicted buffer consumption and Q is elution flow rate used for single column experiments.

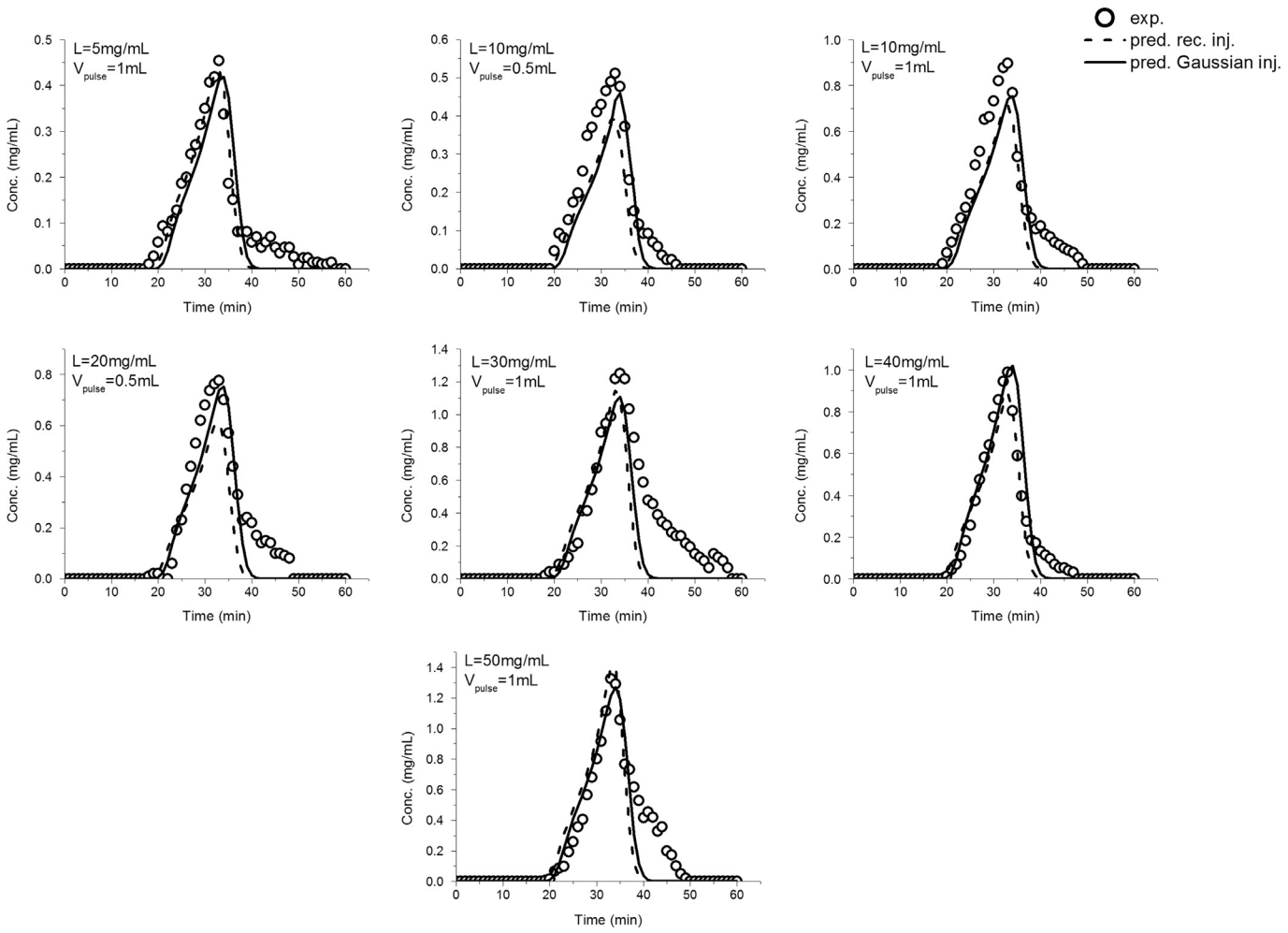

Fig. 3. Experimental vs. predicted elution profile of native refolded lysozyme using both simplified rectangular and experimental injection profiles.

4. Results and discussions

4.1. Single-column batch refolding

When 1 mL of 30, 40 and 50 mg/mL of denatured/reduced lysozyme was refolded on SEC, although no protein signal was observed for aggregates, the refolding yield values (70%, 50% and 40%) suggested formation of insoluble aggregates and in-column precipitation of these species. It was found that aggregation should be only introduced to the model when the local protein concentration exceeds a critical concentration (i.e. solubility of early intermediate species) to predict the results of lysozyme refolding/aggregation on SEC for the concentration ranges used in this work as well as our previous work (described in Section 2.3) (Saremirad et al., 2014b). As illustrated in Fig. 3 the modified model considering a critical concentration and experimental injection profile of the protein provides an improved agreement between experimental and predicted results compared to the model without a critical concentration. The two fitted parameters namely aggregation kinetic constant (k_a) and early intermediate solubility in refolding buffer (C_s) however were found to be correlated and multiple solutions were obtained for minimization problem. Consequently, the solubility of early intermediates was measured experimentally as described in Section 3.7. The above mentioned parameters were $0.05 \pm 2.8 \times 10^{-5}$ mL/mg min and 4.4 ± 0.9 mg/mL respectively.

4.2. Single-column batch refolding of DTT-free lysozyme

The apparent refolding kinetic of DTT-free lysozyme found to be equal to lysozyme refolding with carry-over of DTT within experimental error. It can be seen in Fig. 4 that $k_{app} = 0.08\ \text{min}^{-1}$ adequately predicts the result of DTT-free lysozyme refolding on SEC at loading concentrations of ~5 and 10 mg/mL and 1 mL injection volume. This is because the refolding kinetic constant with DTT carry-over was measured for a system with high dilution factor (~50 times) and the carry-over of reduced DTT was insignificant.

4.3. Model parameters for urea

The experimental mass transfer and equilibrium constants for urea ($k_{ov,urea}$ and $K_{eq,urea}$) were found to be $51.97 \pm 0.02\ \text{min}^{-1}$ and 0.9 ± 0.1. Fig. 5 illustrates the experimental versus predicted urea concentration at the column outlet using experimentally measured mass transfer parameters as well as parameters calculated by available correlations. It was observed that correlations do not provide an accurate prediction of urea elution profile. For this reason, the fitted values of mass transfer parameters were applied to predict the local concentrations of urea through the SMB-SEC columns and at the raffinate stream.

4.4. SMB-SEC model validation

Park et al. (2006) have studied the refolding of DTT-free lysozyme for loading concentration of 1.78 mg/mL in a 1–1–1–1 four zone SMB-SEC. The model developed in this work was used to predict their results based on the experimental conditions used in their work and found to predict the refolding yield and native protein concentration at product outlet within 5.5% and 9.3% respectively. Although the agreement is satisfactory, the model must be tested under various operation conditions such as loading concentrations for further validation. The question is *what should be the criteria for model validation?*

The refolding yield and refolded protein concentration are usually set as model validation criteria. However, simulations for the configuration and operation conditions used in this work (Section 2.2 and Table 1) showed no urea (100% purity) in the raffinate stream, indicating the refolding reaction will continue off-column with the same kinetics as single-column experiments to recover the desired product. Therefore it is suggested that the model is tested against experiments for total soluble protein rather than native refolded protein. It should be noted that in the presence of L-arginine, aggregates precipitate and soluble protein only include early intermediates and native protein conformations. Accordingly, in this work process performance indicators were defined based on total soluble protein (Section 3.9).

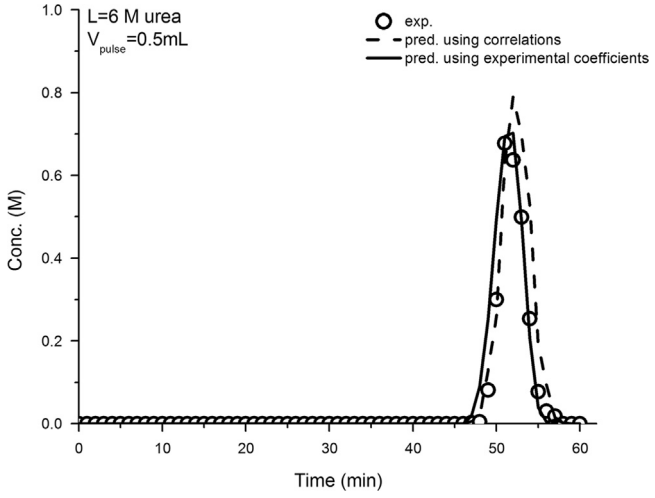

Fig. 5. Experimental vs. predicted elution profile of urea; predicted with the coefficients taken from correlations and coefficients taken from independent experiments.

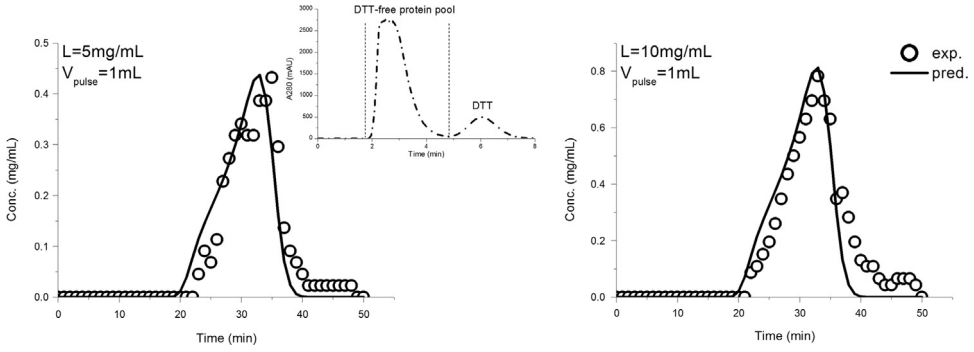

Fig. 4. Experimental vs predicted elution profile of refolded native lysozyme for DTT- free lysozyme loading concentrations of 5 mg/mL and 10 mg/mL; DTT-free lysozyme obtained from desalting column was pooled, concentrated and injected on SEC.

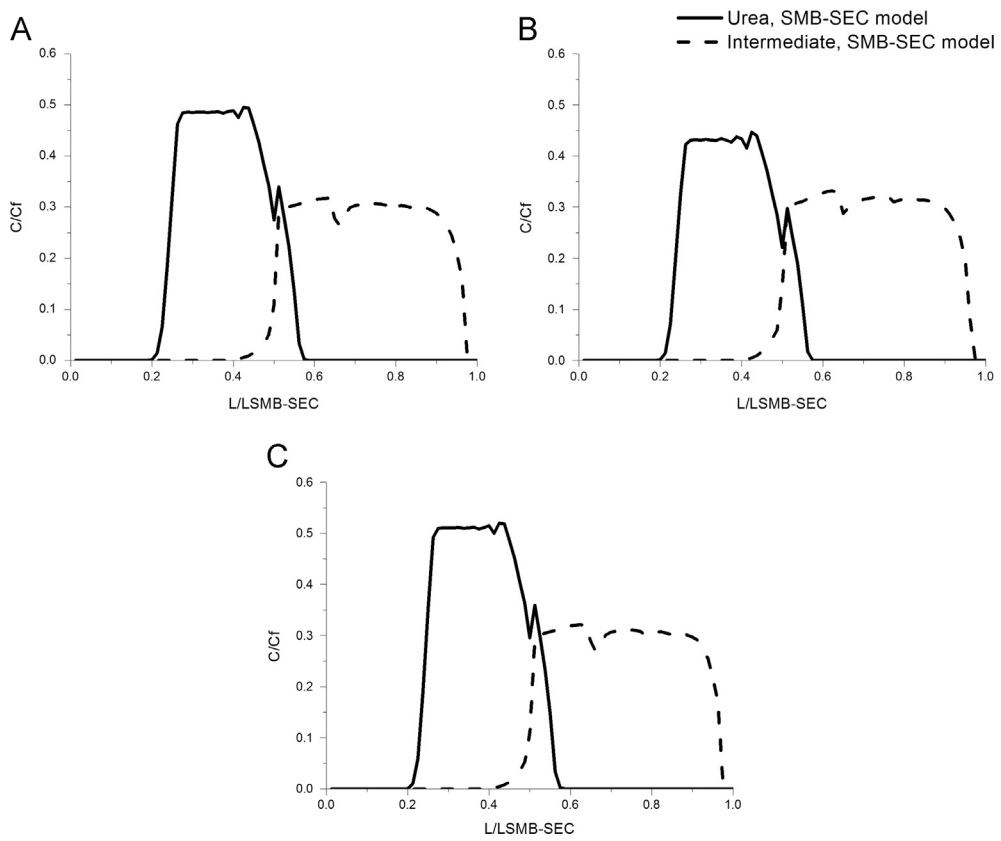

Fig. 6. Mid cycle concentration profiles of urea and early intermediates through SMB-SEC columns for the operating condition reported in Table 1 and 10 mg/mL DTT-free lysozyme; (A) t_s=2.7 min, (B) t_s=3 min and (C) t_s=3.3 min. The number of switching times was fixed at 30 in order to assure steady state operation.

Table 2
SMB-SEC simulations feed concentrations of 5–40 mg/mL, switching time of 3 min and available corresponding SEC experimental results. SEC results are reported for elution flow rate of 1 mL/min and injection volume of 0.5 mL.

$C_{f,U}$ (mg/mL)	$R_{c,pred}$ (dimensionless)	$Pr_{c,pred}$ (mg/mL h)	$Bc_{c,pred}$ (mL/mg)	$R_{b,exp}$ (dimensionless)	$Pr_{b,exp}$ (mg/mL h)	$Bc_{b,exp}$ (mL/mg)
5	1.0	1.6	1.9	1.0	0.1	13.6
10	1.0	3.0	1.0	1.0	0.2	6.8
15	1.0	4.8	0.6	–	–	–
20	0.8	5.4	0.5	1.0	0.3	3.4
40	0.5	6.0	0.5	0.9	0.6	1.9

The next question is *how the model with constant kinetic and thermodynamic parameters will perform in terms of total soluble protein predictions?*

It can be seen from Fig. 6 that there is an overlap between urea and protein concentration profiles. The overlapping area corresponds to the length of two columns in SMB-SEC. Urea possesses different effects on kinetics and equilibrium of refolding/aggregation depending on its local concentration (Volynskaya et al., 2010; Rodriguez-Ropero and van der Veght, 2015; Pan et al., 2014; Xia et al., 2012). Under the current operating conditions, as shown in Fig. 6, over-lapping urea concentration varies between no excess urea compared to the refolding buffer (total urea concentration of 2 M) and about 50% of the urea present in the feed (total urea concentration of about 5 M). Since the model parameters were measured using the refolding buffer during single-column experiments with much higher dilution factor, the developed model with constant kinetic and thermodynamic parameters may over-predict the native protein concentration at SMB-SEC product outlet. This is because lower refolding kinetics and equilibrium in higher urea concentrations is disregarded. Over-prediction of the native protein concentration results in under-prediction of protein aggregation (over-prediction of total soluble protein). However, this error may be balanced by higher solubility of early intermediates and reduced aggregation in higher urea concentrations (Rodriguez-Ropero and van der Veght, 2015, 2015; Xia et al., 2012).

Consequently, further batch experimentation is only required if the model doesn't provide a satisfactory prediction of total soluble protein when SMB-SEC model is tested against continuous refolding experiments. Pan et al. (2014) have reported an experimental approach in order to find appropriate functions to related refolding/aggregation kinetics to urea residual concentrations. Although their work considers different protein model systems than current work, the same approach can be used to incorporate transient refolding environment effects into the model if necessary.

4.5. SMB-SEC performance

Based on above discussion, the developed model was used to study the effect of operating parameters on process performance indicators namely soluble protein recovery and productivity at the raffinate outlet and buffer consumption. Table 2 shows the results of SMB-SEC simulations at operating condition corresponding to

Table 3
SMB-SEC productivity simulations for feed concentrations of 5–40 mg/mL and various operation conditions corresponding to three different switching times used in this work.

$C_{f,U}$ (mg/mL)	t_s (min)	$Pr_{c,pred}$ (mg/mL h)
5	2.7	1.8
10	2.7	3.6
15	2.7	5.4
20	2.7	6.0
40	2.7	7.2
5	3	1.6
10	3	3.0
15	3	4.8
20	3	5.4
40	3	6.0
5	3.3	1.2
10	3.3	3.0
15	3.3	4.2
20	3.3	5.4
40	3.3	6.0

switching time of 3 min in Table 1 for feed concentrations of 5–40 mg/mL. The number of switching times for simulations was fixed at 30 based on mass balance closure which assured steady state condition was reached. The corresponding SEC experimental results are also reported when data was available. It can be seen that, although productivity increases and buffer consumption is reduced at higher feed concentrations, the recovery decreases for concentrations equal and above 20 mg/mL showing aggregation formation; defining an appropriate recovery criterion is crucial to prevent in column precipitation which could deteriorate the packing quality or even block the columns over the time.

As expected the productivity and buffer consumption in SMB-SEC were significantly improved compared to SEC. The buffer consumption can be further reduced by using a closed loop configuration and buffer recycling. For oxidative refolding however, the redox couple ratio might change over time resulting in non-optimal buffer composition. It was previously demonstrated that lysozyme refolds at higher pH values closer to its isoelectric point without the need for redox couple while aggregation was suppressed due to the presence of L-arginine and the refolding yield did not show a significant change (Saremirad et al., 2014a). Based on the characteristics of the protein under study oxidative refolding without the need for a redox couple might offer advantages in terms of chemical cost, buffer preparation and storage.

In order to explore the effect of switching time, the simulations were also carried out for the above feed concentration range and operating conditions corresponding to switching times of 2.7 and 3.3 min. As shown in Table 3, in the studied concentration range switching time of 2.7 min resulted in highest productivity compared to switching times of 3 and 3.3 min and up to 50% improvement was observed for loading concentration of 5 mg/mL, while recovery and buffer consumption did not vary significantly by change of the switching time. The same trend was observed for switching times of 2.7 and 3.3 min in terms of recovery drop for concentrations equal and above 20 mg/mL as switching time of 3 min.

5. Conclusions

This work illustrates important considerations for utilizing single-column data towards design/operation of an SMB process. Our findings showed: (1) at higher local protein concentrations aggregation occurs when local protein concentration exceeds a critical concentration (i.e. solubility of early intermediates); (2) if DTT is to be removed from denatured/reduced lysozyme to avoid further complexity in developing a model and the adverse effect of this reagent on refolding kinetics, the single-column parameters obtained with DTT carry-over are still valid provided they were obtained for a column with high dilution factor; (3) under the operation condition studied, the refolding reaction will continue off-column with the same kinetics as the on-column refolding; (4) as future work SMB-SEC experiments are required to test the model with constant kinetic and thermodynamic parameters against total soluble protein rather than native refolded and one needs to incorporate the effect of dynamic refolding environment by further batch experimentation under various residual urea concentrations only if the above test fails.

Finally the prediction of SMB-SEC performance for loading concentrations of 5–40 mg/mL of DTT-free lysozyme, using the developed model, showed that increasing the concentration increases the productivity and decreases the buffer consumption. However, for concentrations equal to and higher than 20 mg/mL aggregates are formed and precipitate in the column; loading concentrations above 20 mg/mL therefore must be avoided. The operating condition corresponding to lowest switching time resulted in highest productivity and no significant effect on recovery and buffer consumption.

Acknowledgment

Authors would like to thank Dr. Lars Rehmann for stimulating discussions and permission to use analytical lab facilities.

Appendix A. Supplementary material

Supplementary data associated with this article can be found in the online version at http://dx.doi.org/10.1016/j.ces.2015.08.031.

References

Buswell, A.M., Middelberg, A.P., 2003. A new kinetic scheme for lysozyme refolding and aggregation. Biotechnol. Bioeng. 83, 567–577.
Freydell, E.J., van der Wielen, L.A., Eppink, M.H., Ottens, M., 2011. Techno-economic evaluation of an inclusion body solubilization and recombinant protein refolding process. Biotechnol. Prog. 27, 1315–1328.
Freydell, E.J., Bulsink, Y., van Hateren, S., van der Wielen, L., Eppink, M., Ottens, M., 2010b. Size-exclusion simulated moving bed chromatographic protein refolding. Chem. Eng. Sci. 65, 4701–4713.
Freydell, E.J., van der Wielen, L.A., Eppink, M.H., Ottens, M., 2010a. Size-exclusion chromatographic protein refolding: fundamentals, modeling and operation. J. Chromatogr. A 1217, 7723–7737.
Gu, Z., Su, Z., Janson, J.C., 2001. Urea gradient size-exclusion chromatography enhanced the yield of lysozyme refolding. J. Chromatogr. A 918, 311–318.
Goldberg, M.E., Rudolph, R., Jaenicke, R., 1991. A kinetic study of the competition between renaturation and aggregation during the refolding of denatured-reduced egg white lysozyme. Biochemistry 30, 2790–2797.
Huang, C.J., Lin, H., Yang, X., 2012. Industrial production of recombinant therapeutics in *Escherichia coli* and its recent advancements. J. Ind. Microbiol. Biotechnol. 39, 383–399.
Lanckriet, H., Middelberg, A.P., 2004. Continuous chromatographic protein refolding. J. Chromatogr. A 1022, 103–113.
Mazzotti, M., Storti, G., Morbidelli, M., 1997. Optimal operation of simulated moving bed units for nonlinear chromatographic separations. J. Chromatogr. A, 3–24.
Pan, S., Zelger, M., Hahn, R., Jungbauer, A., 2014. Continuous protein refolding in a tubular reactor. Chem. Eng. Sci. 116, 763–772.
Park, B.J., Lee, C.H., Mun, S., Koo, Y.M., 2006. Novel application of simulated moving bed chromatography to protein refolding. Process Biochem. 41, 1072–1082.
Rodriguez-Ropero, F., van der Veght, N., 2015. On the urea induced collapse of a water soluble polymer. Phys. Chem. Chem. Phys. 17, 8491–8498.
Ricchiuto, P., Brukhno, A.V., Auer, S., 2012. Protein aggregation: kinetics versus thermodynamics. J. Phys. Chem. B 116, 5384–5390.
Rajendran, A., Paredes, G., Mazzotti, M., 2009. Simulated moving bed chromatography for the separation of enantiomers. J. Chromatogr. A 1216, 709–738.
Saremirad, P., Wood, J.A., Zhang, Y., Ray, A.K., 2014b. Oxidative protein refolding on size exclusion chromatography at high loading concentrations: Fundamental studies and mathematical modeling. J. Chromatogr. A 1370, 147–155.

Saremirad, P., Wood, J.A., Zhang, Y., Ray, A.K., 2014a. Multi-variable operational characteristic studies of on-column oxidative protein refolding at high loading concentrations. J. Chromatogr. A 1359, 70–75.
Ströhlein, G., Mazzotti, M., Morbidelli, M., 2005. Simulated Moving-Bed Reactors, in: Integrated Chemical Processes: Synthesis, Operation, Analysis, and Control. Wiley-VCH Verlag GmbH & Co., KGaA, pp. 183–201.
Volynskaya, A.V., Murasheva, S.A., Skripkin, A. Yu, Shishkove, A.V., 2010. A lysozyme unfolding mechanism. Dokl. Phys. Chem. 430, 29–32.
Van den Berg, B., Chung, E.W., Robinson, C.V., Mateo, P.L., Dobson, C.M., 1999. The oxidative refolding of hen lysozyme and its catalysis by protein disulfide isomerase. EMBO J. 18, 4794–4803.
Wellhoefer, M., Sprinzl, W., Hahn, R., Jungbauer, A., 2014. Continuous processing of recombinant proteins: Integration of refolding and purification using simulated moving bed size-exclusion chromatography with buffer recycling. J. Chromatogr. A 1337, 48–56.
Wellhoefer, M., Sprinzl, W., Hahn, R., Jungbauer, A., 2013. Continuous processing of recombinant proteins: Integration of inclusion body solubilization and refolding using simulated moving bed size exclusion chromatography with buffer recycling. J. Chromatogr. A 1319, 107–117.
Xia, Z., Das, P., Shakhnovich, E.I., Zhou, R., 2012. Collapse of unfolded proteins in a mixture of denaturants. J. Am. Chem. Soc. 134, 18266–18274.
Zhang, Y., Rohani, S., Ray, A.K., 2008. Numerical determination of competitive adsorption isotherm of mandelic acid enantiomers on cellulose-based chiral stationary phase. J. Chromatogr. A 1202, 34–39.
Zelic, B., Nesek, B., 2006. Mathematical modeling of size exclusion chromatography. Eng. Life Sci. 6, 163–169.